8500–8515 *Nucleic Acids Research, 2018, Vol. 46, No. 16* *Published online 24 July 2018*
doi: 10.1093/nar/gky647

Single molecule kinetics uncover roles for *E. coli* RecQ DNA helicase domains and interaction with SSB

Debjani Bagchi[1], Maria Manosas[2,3], Weiting Zhang[4], Kelly A. Manthei[5], Samar Hodeib[4], Bertrand Ducos[4], James L. Keck[5,*] and Vincent Croquette[4,*]

[1]Physics Department, Faculty of Science, Maharaja Sayajirao University of Baroda, Vadodara, Gujarat - 390002, India, [2]Departament de Física de la Materia Condensada, Universitat de Barcelona, Barcelona 08028, Spain, [3]CIBER-BBN de Bioingenieria, Biomateriales y Nanomedicina, Instituto de Sanidad Carlos III, Madrid, Spain, [4]Laboratoire de physique statistique, Département de physique de l'ENS, École normale supérieure, PSL Research University, Université Paris Diderot, Sorbonne Paris Cité, Sorbonne Universités, UPMC Univ. Paris 06, CNRS, 75005 Paris, France. IBENS, Département de biologie, École normale supérieure, CNRS, INSERM, PSL Research University, 75005 Paris, France and [5]Department of Biomolecular Chemistry, University of Wisconsin Medical School, Madison, WI 53706-1532, USA

Received April 10, 2018; Revised July 01, 2018; Editorial Decision July 05, 2018; Accepted July 15, 2018

ABSTRACT

Most RecQ DNA helicases share a conserved domain arrangement that mediates their activities in genomic stability. This arrangement comprises a helicase motor domain, a RecQ C-terminal (RecQ-C) region including a winged-helix (WH) domain, and a 'Helicase and RNase D C-terminal' (HRDC) domain. Single-molecule real-time translocation and DNA unwinding by full-length *Escherichia coli* RecQ and variants lacking either the HRDC or both the WH and HRDC domains was analyzed. RecQ operated under two interconvertible kinetic modes, 'slow' and 'normal', as it unwound duplex DNA and translocated on single-stranded (ss) DNA. Consistent with a crystal structure of bacterial RecQ bound to ssDNA by base stacking, abasic sites blocked RecQ unwinding. Removal of the HRDC domain eliminates the slow mode while preserving the normal mode of activity. Unexpectedly, a RecQ variant lacking both the WH and HRDC domains retains weak helicase activity. The inclusion of *E. coli* ssDNA-binding protein (SSB) induces a third 'fast' unwinding mode four times faster than the normal RecQ mode and enhances the overall helicase activity (affinity, rate, and processivity). SSB stimulation was, furthermore, observed in the RecQ deletion variants, including the variant missing the WH domain. Our results support a model in which RecQ and SSB have multiple interacting modes.

INTRODUCTION

RecQ DNA helicases are motor proteins that convert the chemical energy of ATP hydrolysis to the mechanical energy required for single-stranded (ss) DNA translocation or double-stranded (ds) DNA unwinding (1). These activities are critical for RecQ's roles in genome maintenance in organisms ranging from bacteria to humans (2,3). In *Escherichia coli*, RecQ is a component of the RecF pathway of recombinational repair, which repairs ssDNA gaps and dsDNA breaks when the main repair pathway, RecBCD, is inactivated by mutation (4). *recQ*–defective *E. coli* with *recBC sbcB* mutations are UV sensitive leading to a decay in recombination frequency that cause cell growth defects and cell death (5,6). *Escherichia coli* RecQ also functions in suppressing illegitimate recombination (7,8), repairing stalled replication forks (9) and promoting induction of the SOS response (6,10,11). In humans, defects in three of the five RecQ proteins (BLM, WRN, RECQ4) give rise to distinct genomic instability and cancer predisposition disorders (12). RecQ helicases from many organisms have been found to function as components in higher-order complexes with heterologous protein partners. In particular, various RecQs interact directly with topoisomerases, single-stranded DNA-binding proteins (SSBs), and replicative polymerases as part of their genome maintenance activities (13–23). Therefore, investigating the activity of RecQ in the presence of other replication, recombination, and repair proteins is crucial for a thorough understanding of the cellular mechanisms of RecQ enzymes.

Most RecQ helicases, including *E. coli* RecQ, contain three evolutionarily conserved domains: helicase, RecQ-C, and 'helicase and RNase D C-terminal' (HRDC) do-

*To whom correspondence should be addressed. Tel: +33 1 44 32 34 92; Fax: +33 1 44 32 34 33; Email: vincent.croquette@lps.ens.fr
Correspondence may also be addressed to James L. Keck. Tel: +1 608 263 1815; Fax: +1 608 262 5253; Email: jlkeck@wisc.edu

main (Figure 1). The helicase and RecQ-C domains form a protease-resistant catalytic core (RecQ-ΔC) that has wild-type levels of DNA unwinding in bulk biochemical experiments but has a reduced affinity for DNA (24). The crystal structures of *E. coli* RecQ-ΔC and HRDC domains have been determined along with the DNA-bound form of the homologous RecQ-ΔC fragment from *Cronobacter sakazaii* (25–27) (Figure 1B and C). In addition, structures of human BLM and RecQ1 have provided insights into RecQ mechanisms (28–32). The helicase activity of RecQ enzymes appears to be governed by the catalytic core domain (2,33,34). Within this portion of the protein, the helicase domain and the RecQ-C domain, comprising Zn^{2+}-binding and winged-helix (WH) domains, are conserved in nearly all RecQ family members. The HRDC is also a well-conserved structural domain, however, it is absent in two human RecQ helicases, and some bacterial RecQ proteins have multiple HRDC domains. The WH domain from *E. coli* RecQ has been shown to bind to *E. coli* SSB, forming a complex with enhanced helicase activity (20). This interaction is mediated by the association of RecQ with the disordered C-terminal tail of SSB (SSB-Ct), which is a common mechanism by which many proteins bind to SSB (35). Recently Mills *et al.* (36) have shown that RecQ can actively displace SSB bound to ssDNA, but it is not clear whether other interaction modes are present between the two proteins.

Here, we have carried out a series of single-molecule experiments to examine the kinetics of *E. coli* RecQ DNA unwinding, the roles of its different domains, and the effects of SSB. Although bulk biochemical (35–38) and structural approaches (24–26) have begun to shed light on these mechanistic questions, experiments at the single molecule level (8,36) have proven to be an excellent complementary tool to traditional studies by examining the action of individual molecules at high spatial and temporal resolution, uncovering dynamic heterogeneities that are lost to ensemble averaging in bulk experiments (39–46). In our studies, the DNA unwinding activity of individual RecQ helicase molecules is monitored in real time by manipulating a DNA hairpin using magnetic tweezers (43,47). These assays reveal that the wild type *E. coli* RecQ (RecQ-wt) displays two distinct kinetic modes: a 'slow', back and forth unwinding mode, similar to the persistent random walk, and a 'normal', uniform speed unwinding mode. When the HRDC domain is removed (in the RecQ-ΔC deletion variant), RecQ exhibits only the normal unwinding mode. Interestingly, strand switching and repeated unwinding are observed when the helicase unwinds the entire hairpin and translocates up to the hairpin loop, showing that RecQ can control its orientation relative to a DNA fork and direct its motion towards unwinding. When the HRDC and WH domains are both removed (in the RecQ-ΔΔC deletion variant), binding affinity for ssDNA is severely compromised (48), but an unexpected unwinding activity with an irregular speed and low processivity is preserved, indicating that the WH domain is not absolutely required for DNA unwinding. Inclusion of SSB enhances the binding and unwinding activity of RecQ-wt and RecQ-ΔC. Surprisingly, SSB also stimulates DNA unwinding by RecQ-ΔΔC, which lacks the previously identified SSB C-terminal tail (SSB-Ct) binding site, and increases its processivity to wild-type levels in a manner that depends upon the presence of the SSB-Ct sequence. This stimulation could be due to an unidentified interaction between SSB and the helicase domain. Moreover, the presence of SSB leads to a new 'fast' mode of DNA unwinding in RecQ-wt and the different RecQ variants, with rates increased by a factor of four, in addition to the 'slow' and 'normal' modes observed in the absence of SSB. This high-velocity rate is not observed in the presence of the SSB-Ct alone but requires the full-length SSB, consistent with both RecQ/SSB and SSB/ssDNA interactions being important for stimulation of RecQ activity. Overall, the results predict a complex RecQ-SSB association involving multiple interaction modes.

MATERIALS AND METHODS

Protein purification

All RecQ variants (Supplementary Figure S1) were overexpressed purified as described previously (24), except for some specific changes detailed in Supplementary Material. SSB variants were purified as described in (49).

DNA substrates

Most of the assays are performed with a hairpin containing 1239 base pairs (bp), with a 4 nt loop, a 76 nt 5′-biotinylated ssDNA tail and a 146-bp 3′-digoxigenin labeled dsDNA tail synthetized as described previously (45). The hairpin is tethered between a 1 μm magnetic streptavidin coated bead (MyOne, Invitrogen), and a glass coverslip treated with anti-digoxigenin (Roche). Some experiments were performed with shorter DNA hairpins (80 or 180 bp in length), synthesized by hybridization and subsequent ligation of specific oligonucleotides (Supplementary Material and Supplementary Figure S2). The stalled replication fork substrate, which is a 500 bp DNA hairpin with complementary dsDNA arms, was generated in the reaction chamber as described previously (46). The denaturation bubble experiment was done on a 17 kb dsDNA (part of the λ-DNA) multiply labeled with biotin and digoxigenin at the two extremities.

Experimental setup

The magnetic bead is held in the tweezers by a pair of magnets that produce a vertical force, typically ranging from 0.01 to 20 pN (Figure 1D). The force is calibrated by the Brownian fluctuations of the tethered bead (47,50). By using this calibration, the pulling force is then adjusted by monitoring the distance separating the magnets from the beads on the coverslip. A 100× 1.2 N.A. microscope objective (Olympus) images the bead onto a CCD camera (Jai) for real-time position 3D tracking at 30 Hz. The image of the bead displays diffraction rings that are used to estimate its 3D position as explained elsewhere (47). The accuracy of the z tracking is 3 nm from one frame to the next and the tracking can be performed simultaneously on 40–50 beads (45). The measured elasticity of ssDNA is used to estimate the number of unwound bp (Supplementary Figure S3).

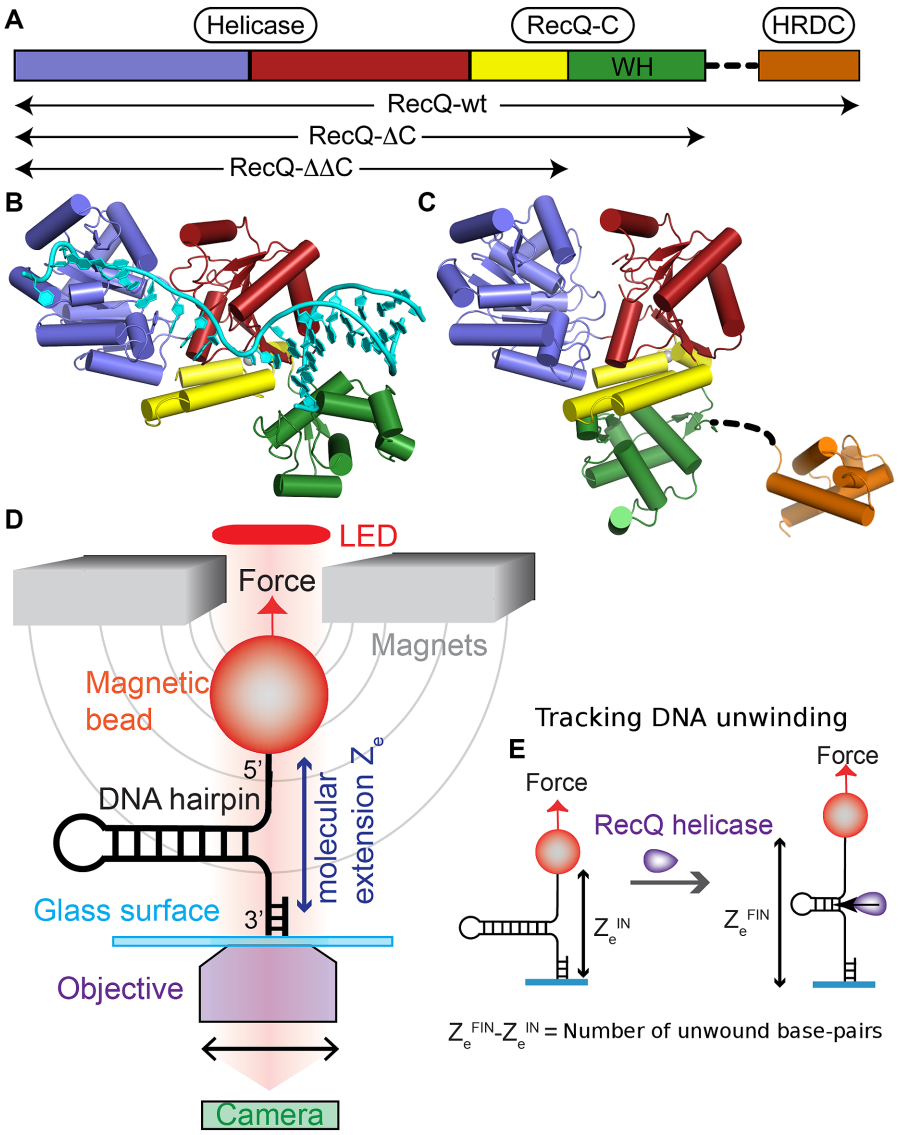

Figure 1. Structure of *E. coli* RecQ and sketch of the single molecule setup. (**A**) Domain organization of *E. coli* RecQ showing the relative sizes of the Helicase (blue and red, for the two RecA-like folds), RecQ-C (yellow (Zn^{2+}-binding domain) and green (winged-helix domain)), HRDC (orange) domains (26). Domains included in RecQ-ΔC and RecQ-ΔΔC used in this study are illustrated. (**B**) Structures of the RecQ-ΔC bound to DNA and (**C**) apo RecQ-ΔC and HRDC domains shown with a linker (dashed line) to emphasize the independence of the two structures. (**D**) Principle of the magnetic tweezers: a DNA hairpin is tethered between a magnetic bead and a glass surface. Force is exerted on the bead by magnets, and its coordinates are tracked by imaging with a camera after magnification by an inverted microscope. (**E**) The extension of the hairpin is recorded with nanometer resolution. When a helicase unwinds the dsDNA part of the hairpin, the extension of the tethered hairpin increases.

Helicase assay

All the experiments were conducted at a temperature of 29 °C, unless otherwise mentioned, with buffer containing 20 mM Tris–HCl pH 7.6, 25 mM NaCl, 3 mM $MgCl_2$, 2% BSA, 0.5 mM DTT and 0.5 mM ATP.

Data analysis

Unwinding rates were found from either linear fit to unwinding events selected manually as in (Figure 2) or by applying a non-linear filter (51) to the entire trace, and then computing its derivative. In the latter case, the rate histogram weighted by the number of base pairs unwound by the helicase in one bin is computed. This process allows to incorporate in the analysis the trace between helicase unwinding bursts since they do not add much (Supplementary Figure S4). Two different approaches were used to measure the translocation rate of RecQ: (i) the hairpin re-annealing signal in the wake of the helicase after the enzyme has passed the apex is used to estimate the enzyme translocation (Supplementary Figures S5 and S6). (ii) The translocation rate is also deduced from the difference in $Z(t)$ occurring before and after applying a force burst ($F_{open} > 15$ pN) to the molecule to transiently unfold the hairpin in the course of an unwinding event (Figure 3A). The unwinding/translocation velocity for each force is computed as the mean of the Gaussian fit to the distribution of unwinding/translocation velocity, calculated

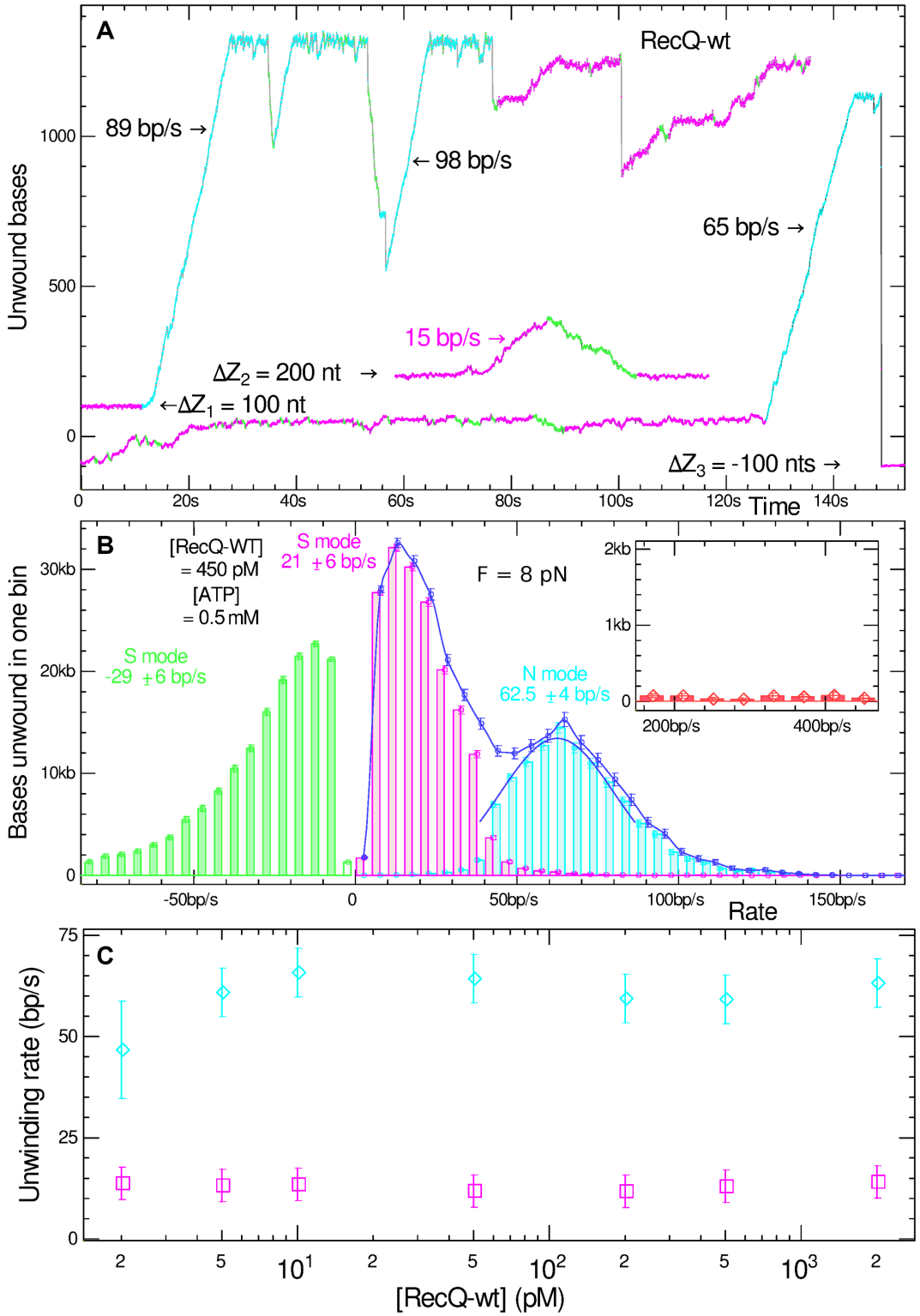

Figure 2. Unwinding results concerning RecQ-wt. (**A**) Unwinding events of RecQ-wt illustrating the S mode (in green and magenta), with pauses, instantaneous re-zipping and occasional bursts of N mode (in cyan). Unwinding events may start in the S mode and switch to the N mode or *vice versa*. The repeated unzipping-rezipping events near the hairpin apex in the cyan traces illustrate the ability of RecQ to maintain the unzipped state of the hairpin in its N mode. The magenta trace presents a strand switching event occurring at $t = 88$ s. Conditions used are [ATP] = 0.5 mM, [RecQ-wt] = 1 nM, $T = 29$ °C and $F = 8$ pN. (**B**) The histogram of the RecQ-WT rate, which includes the number of bases unwound or translocated per second, RecQ-WT is dominated by its diffusion mode. The insert indicates that there is basically no helicase activity at high rates. (**C**) Speed of the N (cyan) and S (magenta) modes as a function of [RecQ-wt].

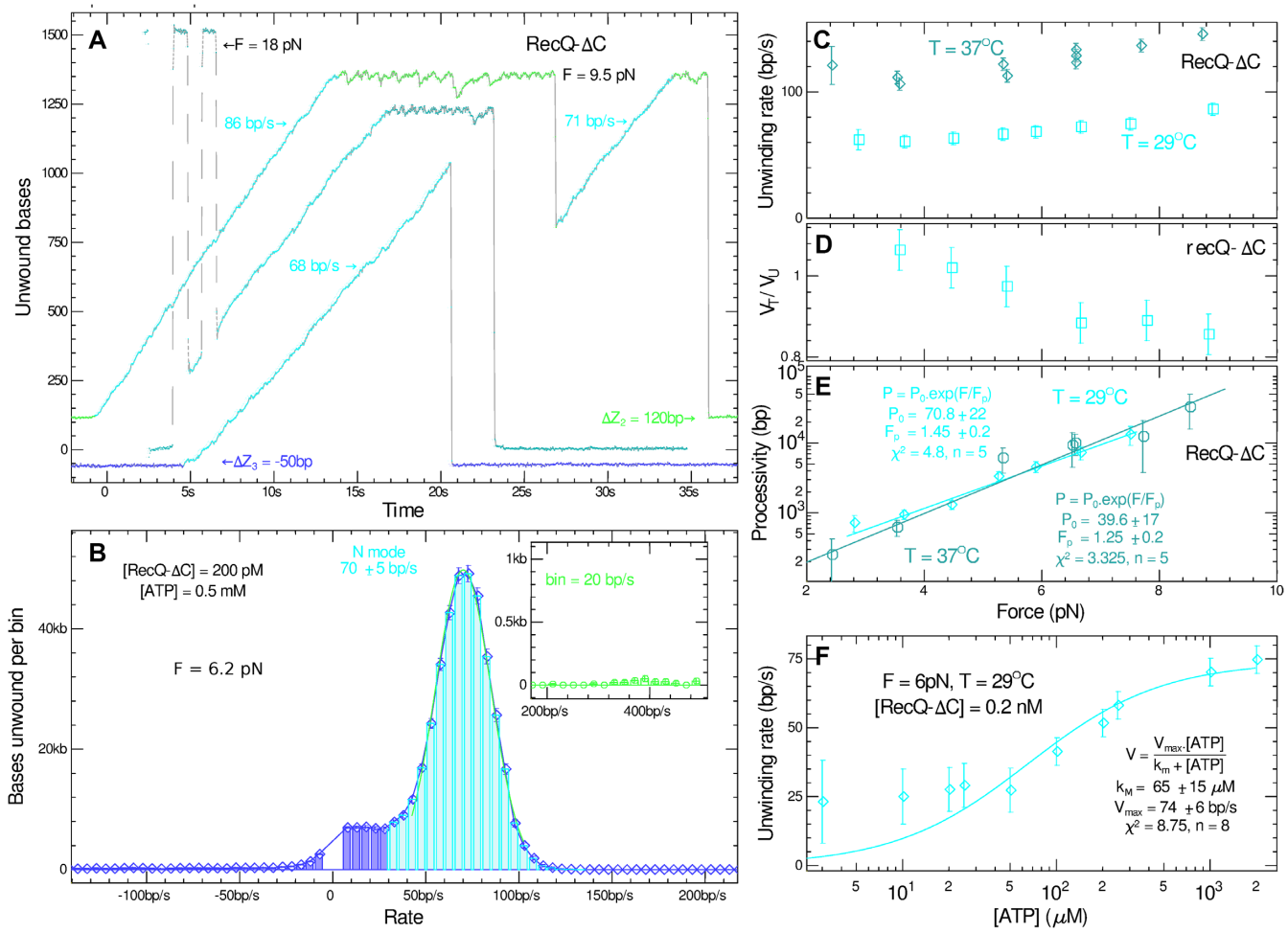

Figure 3. Unwinding results concerning RecQ-ΔC. (**A**) Unwinding events of RecQ-ΔC, illustrating that the helicase only work in the N mode. The lowermost trace—unwinding abruptly stops and hairpin rezips upon helicase dissociation. Middle trace–RecQ binding and unwinding is triggered after mechanically unzipping the hairpin for 1 s at 18 pN, a second opening of the hairpin reveals enzyme translocation along ssDNA. Upon decreasing force to 9.5 pN, RecQ-ΔC resumes unwinding and once the hairpin is fully open, RecQ-ΔC maintains the hairpin open in an active process by repeated strand switching until the enzyme dissociates. The green event of the topmost trace exhibits a similar phenomenon except that enzyme dissociation is followed by unwinding by another helicase. This last event could also be a slippage of RecQ-ΔC over a finite distance. Conditions used are [ATP] = 0.5 mM, [RecQ-ΔC] = 400 pM and $T = 29$ °C. (**B**) Unwinding speed histogram for RecQ- ΔC presenting a very clear unwinding mode. (**C**) Unwinding rates of RecQ-ΔC as a function of force at two different temperatures. (**D**) Ratio of the translocation to the unwinding speed of RecQ-ΔC versus force. (**E**) RecQ unwinding rates and processivity versus force for [RecQ-ΔC] = 200 pM, [ATP] = 0.5 mM. The processivity is calculated by fitting an exponential function of the force to the experimentally obtained values. The fit parameters and results are shown the figure, with P_0 being the processivity at 0 pN force, F_p the force increment leading to an increase of e (= 2.71) in processivity and χ^2 the classical normalized deviation between experimental data points and the exponential model. (**F**) ATP dependence of the unwinding speed of RecQ-ΔC versus [ATP] at $F = 6$ pN and [RecQ-ΔC] = 200 pM. The kinetics exhibited fits well with the Michaelis–Menten kinetics with the Michaelis constant k_M shown in the figure.

from typically 50–400 events. Due to the uncertainty in the force measurement, the total error in the estimation of the unwinding/translocation velocity is the sum of the statistical error and the error in the conversion from extension to bp done using ssDNA elasticity.

RESULTS

Single-molecule RecQ-mediated DNA unwinding studies illustrate the role of RecQ domains

In order to measure the rates of DNA unwinding catalyzed by wild type RecQ and truncated RecQ variants at the single molecule level, we used a 1.2 kb hairpin substrate tethered between a glass cover slip and a magnetic bead that is pulled by a pair of magnets (Figure 1D and E). By adjusting the position of the magnets, the force applied to the hairpin is controlled while the bead position is monitored allowing measurements of the extension of the DNA molecule with ∼3 nm accuracy (47). In the presence of a helicase and ATP, unwinding events are detected as an increase in the DNA molecular extension, since for each base pair (bp) unwound two nucleotides of ssDNA are released (typically 1 nm for 1 bp unwound at 10 pN). Extension changes are converted to the number of unwound bp by using the previously measured ssDNA elasticity (Supplementary Figure S3). To ensure that each unwinding event corresponds to the activity of a single enzyme complex, enzyme concentrations were kept low such that DNA unwinding bursts are rare, with

the time lag between events being ten times larger than the typical duration of a single event. This concentration is typically 100–300 pM for RecQ-wt and RecQ-ΔC and 1 nM for RecQ-ΔΔC. The assay avoids DNA re-annealing in the wake of the helicase by pulling both strands apart with a force much lower than the DNA unzipping threshold. SSB is the classical partner of helicases, which slows down DNA re-annealing by sequestering ssDNA. Our assay allows us to quantify the effect of SSB, which does not prevent re-annealing but just slows it down.

RecQ-wt displays complex behavior with a large range of unwinding rates and processivities (Figure 2 and Supplementary Table S1). Some unwinding events occur with a uniform rate, denoted as the 'normal (N) mode' (shown in light cyan traces in Figure 2A) whereas other events present a slower and non-uniform unwinding rate denoted as the 'slow (S) mode' (shown in light magenta traces in Figure 2A). This bimodal behavior has not been previously identified in ensemble assays. The N mode is characterized by a uniform rate of 62 ± 4 bp/s at saturating ATP and 29 °C (90 ± 4 bp/s at 37 °C), whereas the S mode unwinding is characterized by frequent pauses and backtracks in an apparent persistent random walk at a rate of 15–25 bp/s at 29 °C (Figure 2B and C). Interestingly, ensemble assays with RecQ-wt reported an unwinding rate of 30 bp/s (52,53), a value that is intermediate to the S and N regimes suggesting that the bulk-experiment measured rate is an ensemble average of the two regimes. Individual helicases can switch between the two modes within a single event (Supplementary Figure S7). RecQ-wt can also pass the loop apex of the DNA hairpin and continue translocating on the ssDNA produced by unwinding. In this case, the extent to which the hairpin refolds is dictated by the position of the helicase, which blocks DNA reannealing at the enzyme position (42). The processivity and rate of RecQ-wt DNA unwinding are difficult to analyze owing to its bimodal behavior. In the N mode, RecQ-wt is highly processive and can unwind the 1.2 kb hairpin completely, but the overall processivity is restricted by random switching to the S mode. In two recent publications (8,36), similar rates and behaviors have been reported. For RecQ-wt, Harami *et al.* (8) find a rate of 82 ± 1 bp/s close to our findings. The authors reported the complex behavior of RecQ-wt but did not define the existence of two rates.

To examine the impact of removing the HRDC domain, RecQ-ΔC was tested using the same single-molecule assay. RecQ-ΔC displays a unimodal sustained unwinding activity (Figure 3). The mean unwinding rate 74 ± 6 bp/s at 29 °C from Figure 3C (values vary slightly between Figure 3B, C and F and Supplementary Table S1, but remain compatible within their error bars) and 140 ± 6 bp/s at 37 °C seems to be slightly faster than the N-mode of the RecQ-wt, is independent of the applied force (Figure 3C), and nearly matches the measured ssDNA translocation rate for RecQ-ΔC (Figure 3D). These results are a signature of an active mechanism of unwinding as previously discussed (44). The S mode observed with RecQ-wt was not detected with RecQ-ΔC. We took advantage of the unimodal behavior of RecQ-ΔC to investigate its ATP-dependent rate and processivity. The processivity of RecQ-ΔC increases exponentially with the applied force as $P \sim P_0 \exp(F/F_p)$ (Figure 3E), exceeding 4 kb above 6 pN. At the lowest forces studied (about 4 pN), the processivity is still 1 kb and extrapolation to zero force (as expected *in vivo*) gives ≈ 50 bp ($P_0 = 70$ bp at 29 °C and $P_0 = 39$ bp at 37 °C). The measured unwinding rate value agrees with the 70 bp/s measured in the ensemble assays (38). ATP titration assays showed that RecQ-ΔC N-mode unwinding fits well with first order Michaelis–Menten kinetics, with $K_M = 65 \pm 15$ μM and $V_{max} = 74 \pm 6$ bp/s (Figure 3F). At low ATP concentrations, unwinding bursts are sporadic and are characterized by pauses, slippages, and short rewinding events. At ATP concentrations below the K_M, pauses are common, especially when the helicase encounters GC rich regions of the substrate. This sequence sensitivity is also present at saturated ATP concentrations. However, the helicase does pass these GC barriers quite often (Supplementary Figure S8). Similar unwinding rates and pausing at GC-rich DNA were observed in earlier single-molecule studies (8,36).

Given the roles for the WH domain in DNA binding (54) and in DNA unwinding (31,32,55), we next examined the impact of removing the WH domain from RecQ-ΔC. Surprisingly, RecQ-ΔΔC, the RecQ variant lacking both the WH and HRDC domains, can also unwind dsDNA (Figure 4) as was also shown in (8). The unwinding rate for RecQ-ΔΔC is variable, with an average of ∼60 ± 20 bp/s (Figure 4A and B), and a limited processivity of ∼12.5 bp at $F =$ 8 pN (Figure 4C). Its unwinding activity is best observed when a substantial force (typically 10 pN) is applied to the ends of the hairpin to assist unwinding. This activity is explored further in subsequent sections.

Strand switching by RecQ and maintenance of the unwound DNA hairpin structure

Single molecule assays have revealed that many non-hexameric helicases can switch the DNA strands on which they translocate, performing the equivalent of a U-turn on dsDNA (41,56,57). Such helicases are believed to translocate through an inchworm mechanism involving alternating binding between two DNA sites during unwinding; the two DNA strands at the fork junction are in contact with the helicase and one binding site might associate with the wrong strand inducing a strand switch (41,57). Notably, the forces opposing helicase translocation during unwinding can actually help to promote its movement when the enzyme's directionality has reversed. Therefore, strand switching leads to hairpin reannealing as the helicase translocates away from the fork that can be observed in our assays as the reversal of the slope of the DNA extension trace (Figure 2A).

The direction reversal of the helicase observed during strand switching is also seen when the helicase unwinds a hairpin and passes the apex region - the hairpin then spontaneously rezips. Such events are not pure strand switching. *Bona fide* strand-switches occur upon unwinding before the helicase reaches the apex, leading to smaller triangular traces. Direction reversal can also be seen while the helicase translocates, leading to a new unwinding event (Figure 2A), but in this case it is difficult to ensure that a single enzyme is involved. In previous studies, we have observed several helicases unwinding a hairpin and continuing their travel by translocating on ssDNA: gp41 (43), UvrD (42) and UPF1

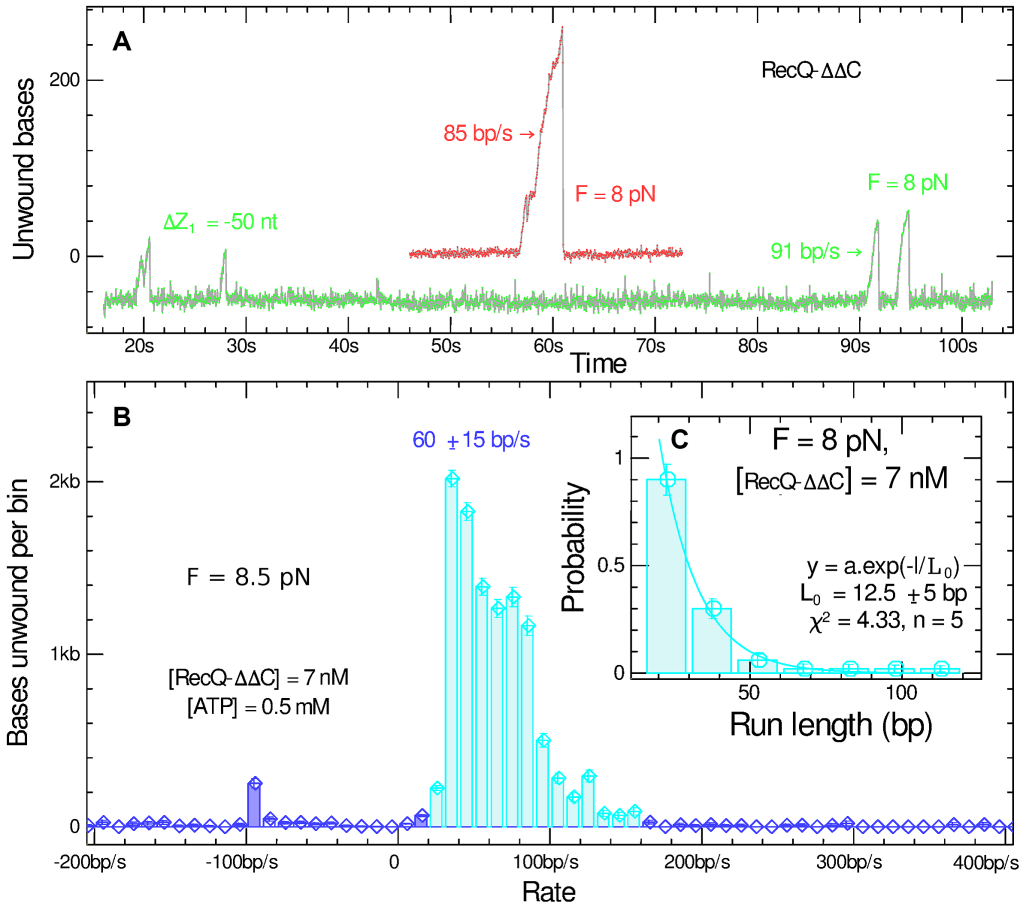

Figure 4. Unwinding results concerning RecQ-ΔΔC. (**A**) Unwinding events observed with RecQ-ΔΔC. The majority of events (green) have a very low processivity, and irregular speed with some exceptions (red). Condition used are [RecQ-ΔΔC] = 7 nM, [ATP] = 0.5 mM, $T = 29$ °C and $F = 8$ pN. (**B**) Histogram of the rates of unwinding of RecQ-ΔΔC. (**C**) Processivity histograms for RecQ-ΔΔC with the probability of an event to unwind over some run length.

(58). RecQ displays a distinct behavior: as it unwinds, upon arriving at the hairpin apex, we cannot see RecQ translocating. RecQ does not fall off its substrate but instead presents an apparent frustrated movement that maintains the hairpin in an unwound state. Two possibilities may explain this process: (i) a small periodic slippage of the helicase triggered by arriving at the apex or (ii) a multitude of strand-switches occurring when the dsDNA fork reforms on the helicase wake. The results shown in Supplementary Figure S5C suggests that this last explanation is the correct one. Thus RecQ presents a strong propensity to stop the translocation motion by performing a strand-switch and resuming unwinding repeatedly.

The strand-switching behavior was observed with RecQ proteins that contain a WH domain (RecQ-wt and RecQ-ΔC) but not in the variant lacking the WH domain (RecQ-ΔΔC). The histograms of the helicase rate in Figures 2B and 3B demonstrate that the unwinding peak has no corresponding peak at negative rates associated with translocation. RecQ-wt and RecQ-ΔC in the N mode typically achieve about 2 strand-switches per second while they maintain an open hairpin structure during a few tens of seconds, due to repeated strand switching activity (see the top part of traces in Figures 2A and 3A). This behavior is RecQ specific. Strand switching statistics are provided in Supplementary Table S2.

A simple explanation for this behavior is that, as observed in the RecQ/DNA structure (25, Figure 1), the WH domain participates in fork recognition and proper orientation of the enzyme on DNA. This fork sensing ability has been also reported in other RecQ helicases (59,60). Such an asymmetric pattern leads to productive and directional DNA unwinding. The activity bursts for RecQ-ΔC and the N mode of RecQ-wt thus present a consistent, well-defined rate of unwinding followed by a plateau when the hairpin is fully open, resulting in a series of rapid strand switching (Figures 2A and 3A and Supplementary Figure S5 and S6), ending with an abrupt hairpin re-hybridization when the enzyme dissociates. In the S mode, RecQ-wt performs a random forward-backward motion, which is difficult to quantify. However, owing to the helicase 3′-5′ directionality, this random movement can be a result of frequent strand switching (Figure 2A). In contrast, RecQ-ΔΔC does not strand switch, and the unwinding events end before the helicase reaches the apex, by an abrupt re-hybridization of the hairpin after helicase dissociation. The absence of strand switching in RecQ-ΔΔC traces might be a result of its low processivity (Figure 4A–C). Alternatively, it could be that the WH

domain that is missing in RecQ-ΔΔC is required to anchor the protein during strand switching.

RecQ translocation on ssDNA

To observe RecQ translocation on ssDNA, a force surge was applied for a short time to transiently open the hairpin when RecQ was actively unwinding DNA (Figure 3A and Supplementary Figures S5, S9 and S10). RecQ translocation cannot be directly observed when the DNA is mechanically unwound, but, by comparing molecular extension measured just before the opening phase and just after the relaxation phase, RecQ translocation can be indirectly detected. As illustrated in Figure 3A (trace with force surge at 18 pN), RecQ-ΔC translocates on the ssDNA template at a speed similar to which it unwinds dsDNA. The low enzyme concentration ensures that this event is the action of a single enzyme or enzyme complex. By repeatedly applying force surges in a periodic fashion we can infer how RecQ behaves on ssDNA (Figure 5). With the RecQ-wt enzyme, a memory effect is observed: if the enzyme is unwinding dsDNA in its N or S mode, translocation along ssDNA occurs mostly with the N or S rate respectively (Figure 5A, B and Supplementary Figure S10). The slow diffusive mode is, however, predominant for RecQ-wt (Figure 5C-D). For RecQ-ΔC the only the normal mode is observed (Figure 5E, F). We have measured the RecQ-ΔC averaged translocation rate at different forces. A comparison of the unwinding and translocation rates of RecQ-ΔC shows that both rates are comparable at all forces (Figure 3D). These results are in agreement with previous single molecule measurements (44). The measured rates for RecQ-wt are also consistent with recent ensemble results (52,53).

The S mode of RecQ-wt

RecQ-wt exhibits an ATP-dependent S mode that presents a diffusive behavior (Figure 5A and B). The diffusive unwinding regime is characterized by a diffusion coefficient, D, in the range of 200 ± 50 nt^2/s from a direct measure of unwinding traces (Figure 5C and D). This behavior has been reported recently for *Arabidopsis thaliana* RecQs with similar diffusion constants (57). Interestingly, this diffusive behavior is also observed for *E. coli* RecQ during ssDNA translocation. In order to characterize the ssDNA translocation in the S mode, we applied force surges with different time duration for the open phase, T_{open}, and we measure the helicase displacement (Figure 5D and Supplementary Figure S10). Applying this assay to RecQ-ΔC reveals just a simple translocation behavior (Figure 5E and F). As expected for a diffusive regime, we find a linear relation between the mean square displacement and T_{open} with almost the same diffusion coefficient ($D = 280 \pm 40$ nt^2/s) found in the unwinding S mode (Figure 5C and D). Similar diffusion constants have been reported for SSB on ssDNA (61,62) and for the cytosine deaminase (63). During an activity burst, the unwinding rate of the enzyme switches between the N and S modes in a random manner (Supplementary Figure S7) suggesting that the same enzyme participates in both modes. The HRDC is necessarily involved in the S mode of unwinding since the diffusive regime is only detected in RecQ-wt. We hypothesize two possible scenarios to explain this behavior: (i) The two modes could be the result of two different arrangements of the HRDC domain as proposed by Harami *et al.* (8) with one mode where HRDC could interact the displaced ssDNA, and the switch between the two enzyme conformations would be the result of the switch between the two modes. (ii) The two modes could be associated with different active oligomeric states, as seen for UvrD (64).

RecQ interacts with DNA nucleotides more strongly during unwinding than during translocation

A recent structure of a bacterial RecQ bound to DNA indicates that a loop within the helicase domain binds to ssDNA by base stacking (Figure 1, (26)). This model predicts that abasic ssDNA would block RecQ translocation and unwinding if the abasic site is present on the 3′ ssDNA strand along which RecQ translocates. To test this model of RecQ translocation, we designed two 80 bp hairpins (Supplementary Methods) that position abasic sites 10 bp away from the loop, on either the bound or displaced strand (Figure 6). The presence of abasic sites on the 3′ template strand stalls the RecQ-ΔC unwinding, which leads to dissociation of the enzyme. In contrast, when the abasic sites are on the displaced strand, RecQ-ΔC is able to unwind through the abasic site region but can still encounter the lesion in its post-unwinding translocation mode. In this situation RecQ-ΔC often passes the abasic sites and translocates further on ssDNA. However, this translocation motion is often interrupted by strand switching or dissociation (Figure 6). Thus, an abasic site efficiently blocks RecQ-ΔC from unwinding DNA but its ability to induce pausing is less efficient for RecQ-ΔC translocating on ssDNA. This assay is only feasible for RecQ-ΔC, which presents a well-defined unwinding rate.

RecQ actively unwinds a three-way junction and rarely reverts the fork

To test for possible functions of *E. coli* RecQ on DNA replication fork structures, we examined its unwinding activity on a three-way junction fork structure consisting of a partially replicated DNA hairpin (46). Biochemical studies have suggested that RecQs are involved in Holliday junction migration (65). Although this substrate lacks ssDNA, RecQ-wt helicase unwinds this substrate with similar rates (59.75 ± 13 bp/s at 6.0 pN, $n = 11$) observed for unwinding the hairpin substrate (Supplementary Figure S11). The unwinding activity is greatly reduced for RecQ-ΔC, which does not load on this substrate efficiently. Interestingly, in rare instances, RecQ-wt was able to revert the substrate into a Holliday junction structure, but with a reduced processivity of a few tens of bp. The fork structure is immediately recovered, assisted by the action of RecQ. These data are consistent with a role for *E. coli* RecQ in regressing DNA forks and forming Holliday junction structures.

RecQ activity in the presence of SSB

RecQ proteins from bacteria and eukaryotes have been shown to directly interact with SSB proteins (17–

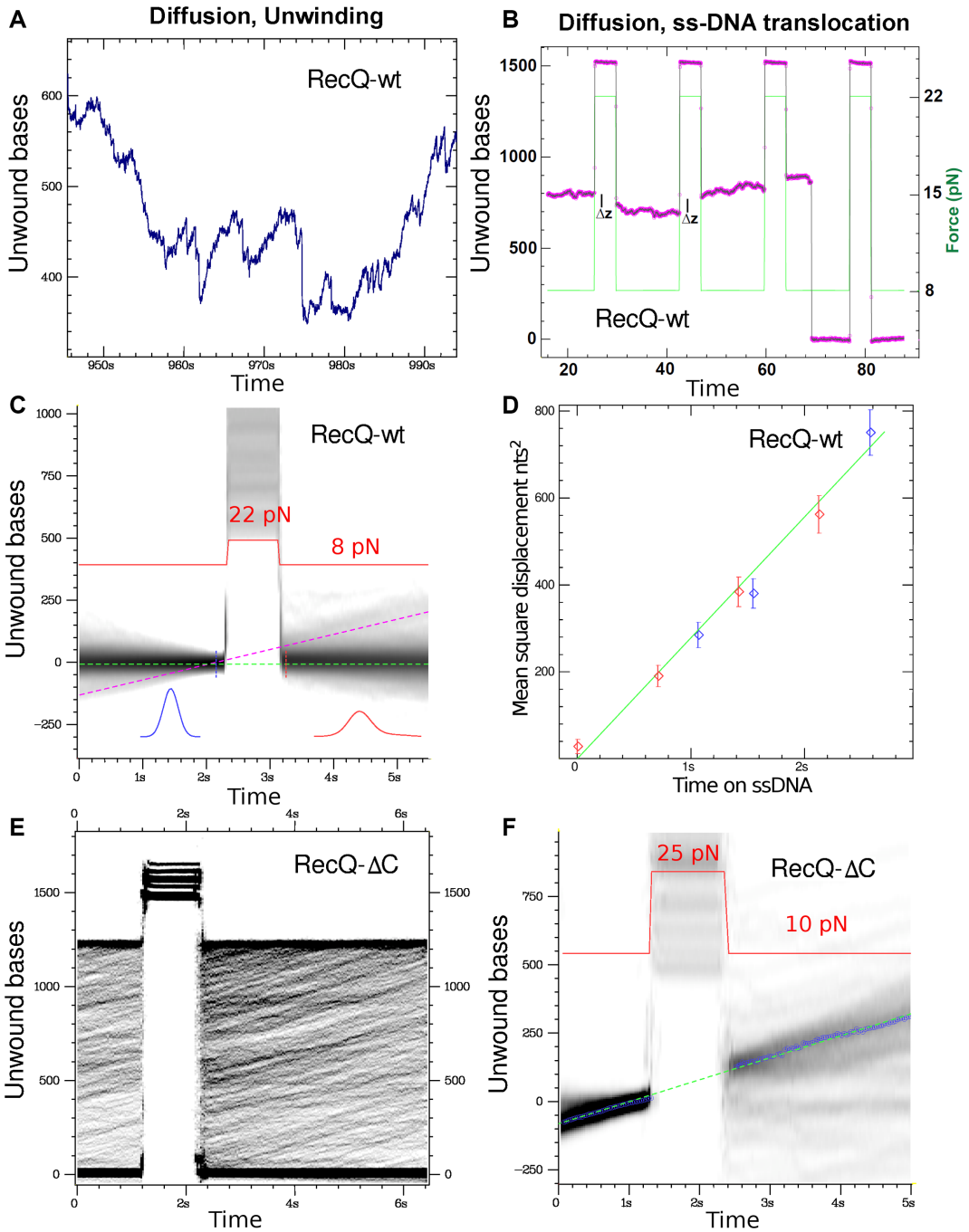

Figure 5. Translocation and diffusion of RecQ. (**A**) Unwinding trace for RecQ-wt in the S mode ($F = 8$ pN, [RecQ-wt] = 80 pM and [ATP] = 0.5 mM). While unwinding, RecQ-wt goes forward and backward in a random manner. (**B**) To probe the helicase translocation activity on ssDNA we repeatedly open and close the hairpin at low protein concentration ([RecQ-wt] = 80 pM) so that the signal just before and after the opening burst is most likely due to the same enzyme. The experimental trace shows a few force cycles with RecQ-wt bound to DNA, working in S mode both during unwinding and during translocation. To better characterize the ssDNA translocation, we averaged a large number of recordings presenting an open burst. (**C**) Event density histogram map of RecQ-wt ([RecQ-wt] = 80 pM) for 2,200 active traces from 17,259 traces from 40 beads of RecQ-wt are shown with their positions readjusted to coincide at t = 2.1 s. Most of the events correspond to the S mode, and the diffusive behavior of RecQ translocation on ssDNA is illustrated by the broadening of the histograms from just before the burst (in blue) to just after (in red). In particular, the traces close to the magenta dashed line corresponds to RecQ-wt working in N mode for 50 events. (**D**) By varying the duration of the open phase, we observe that the broadening of the histogram in (C) corresponds to a diffusive mode both during unwinding (red points) or ssDNA translocation (blue points). RecQ-wt exhibits a diffusive behavior, which is absent in RecQ-ΔC. In (**E**) and (**F**), we show the event density histogram map for RecQ-ΔC ([RecQ-ΔC] = 100 pM), the grey level of the image scales as the log of the histogram density to better visualize the rare events. (E) Superposition of 2048 raw traces of 12 beads. In (F), 121 traces excluding either the fully closed or open hairpin have been shifted so that they all pass by 0, just four frames before the open burst. Most traces show that the helicase which was unwinding had been translocating on ssDNA during the open phase.

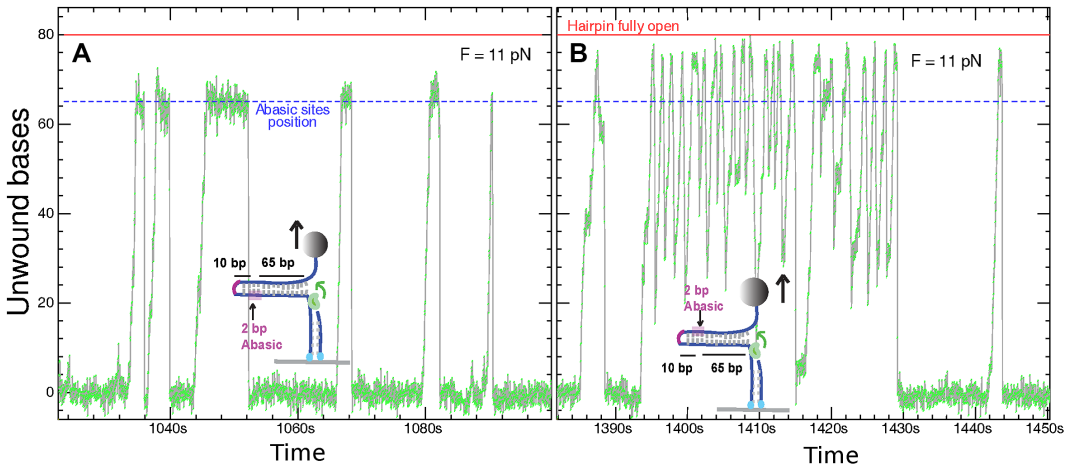

Figure 6. Effect of abasic sites on translocation and unwinding. We used two hairpins having two abasic sites near the loop: on the bound (**A**) and on the displaced strand (**B**). The traces on the left panel show that RecQ-ΔC is unable to pass the abasic sites when the enzyme is unzipping the dsDNA. On the other hand, if the abasic site is on the displaced strand, the enzyme unwinding is unaffected (B). In this condition, the traces pass the maximum extension corresponding to the loop apex, and the enzyme crosses the lesion while translocating on ssDNA (corresponding to the decreasing edge of the signal) with the refolding hairpin pushing the helicase from behind. Strand switching during translocation is slightly affected near the lesion and is more probable further away from the lesion, with RecQ-ΔC reverting back to its unwinding mode leading to a new signal increase. The experimental conditions used are: [RecQ-ΔC] = 200 pM, [ATP] = 0.5 mM.

19,21,22,55). These interactions have been proposed to stimulate RecQ helicase activity and increase its target efficiency to ssDNA/SSB cellular substrates. A recent study proposed an interesting mode of action where RecQ displaces SSB from ssDNA (36). We have expanded our single-molecule studies of RecQ to investigate the effects of SSB on RecQ DNA translocation and unwinding. We first examined SSB binding to our hairpin substrate by investigating how SSB affects reannealing of the hairpin (Supplementary Figure S12). In the absence of SSB below 12 pN, the hairpin anneals faster than the time resolution of our instrument, but in the presence of SSB reannealing is slowed significantly. The reannealing speed in the presence of SSB decreases from 1200 bp/s at 6 pN to few bp/s at 12 pN. We therefore analyzed the impact of SSB on RecQ at moderate forces (9 pN or lower) where reannealing in the presence of SSB can be easily distinguished from the slow re-zipping generated by the translocation of the RecQ enzyme.

Escherichia coli SSB interacts with RecQ using the conserved and structurally dynamic SSB C-terminal sequence (SSB-Ct, Met-Asp-Phe-Asp-Asp-Asp-Ile-Pro-Phe) (22). In order to investigate how RecQ helicase activity is affected by SSB, we performed assays with *E. coli* SSB-wt and SSB variants that contain single residue changes in the SSB-Ct that block complex formation with RecQ (22). These include a variant that lacks the C-terminal Phe residue (SSB-ΔC1) and a second variant that substitutes a Ser for the penultimate Pro (SSB-113). The activity of RecQ in the different conditions assayed was characterized by using a single-molecule effective affinity constant defined as: $K_A = T_{exp}[c]/T_{active}$, where T_{exp} and T_{active} are respectively the total time of the assay and the time in which the enzyme is actively unwinding the DNA and [c] is the concentration of the RecQ enzyme. We choose this form of K_A since T_{active} should be roughly proportional to [c] and thus K_A should not be sensitive to the helicase concentration. This affinity constant represents the concentration at which the enzyme is active 100% of the time (e.g. $T_{active} = T_{exp}$). Note that K_A integrates the effect of both binding affinity and enzyme processivity. Therefore, conditions leading to larger K_A might correspond to an increase in the binding affinity of the enzyme to the DNA fork or/and an increase in the unwinding processivity of the enzyme. In order to compare the activity of RecQ alone and in the presence of the different SSB variants, we report the ratio of the affinity constants in the absence and presence of SSB: $K_A^{RecQ(wt,\Delta,\Delta\Delta)}/K_A^{RecQ(wt,\Delta,\Delta\Delta)+SSB}$, with a value <1 corresponding to an inhibitory effect and a value >1 corresponding to an enhancement effect.

The addition of SSB in our single-molecule assay increased unwinding activity of the RecQ-wt, with $K_A^{RecQ\text{-}wt}/K_A^{RecQ\text{-}wt+SSB} = 1.33$ (Figure 7A, B and Supplementary Table S3). *Escherichia coli* SSB variants with single residue changes in the SSB-Ct failed to stimulate RecQ and even diminished the activity, since these SSBs may compete with the helicase for loading on ssDNA (Supplementary Table S3). Therefore, RecQ/SSB complex formation appears essential for SSB stimulation. Similar overall results have been observed in bulk biochemical studies (21). In a similar approach Mills *et al.* (36) have used [SSB] and [RecQ] concentration in the range of 500 nM without ATP and very low SSB concentration (50 pM) with ATP. Our findings explore an SSB concentration in between these two cases with a low RecQ concentration to maintain single molecule conditions. Our results agree with Mills *et al.* (36) in the low concentration limit.

Interestingly, our studies reveal a second feature that could help explain how SSB stimulates RecQ activity: SSB induces a previously unobserved faster kinetic phase in RecQ DNA unwinding and translocation (Figure 7C). When SSB is included, RecQ-wt displays three possible

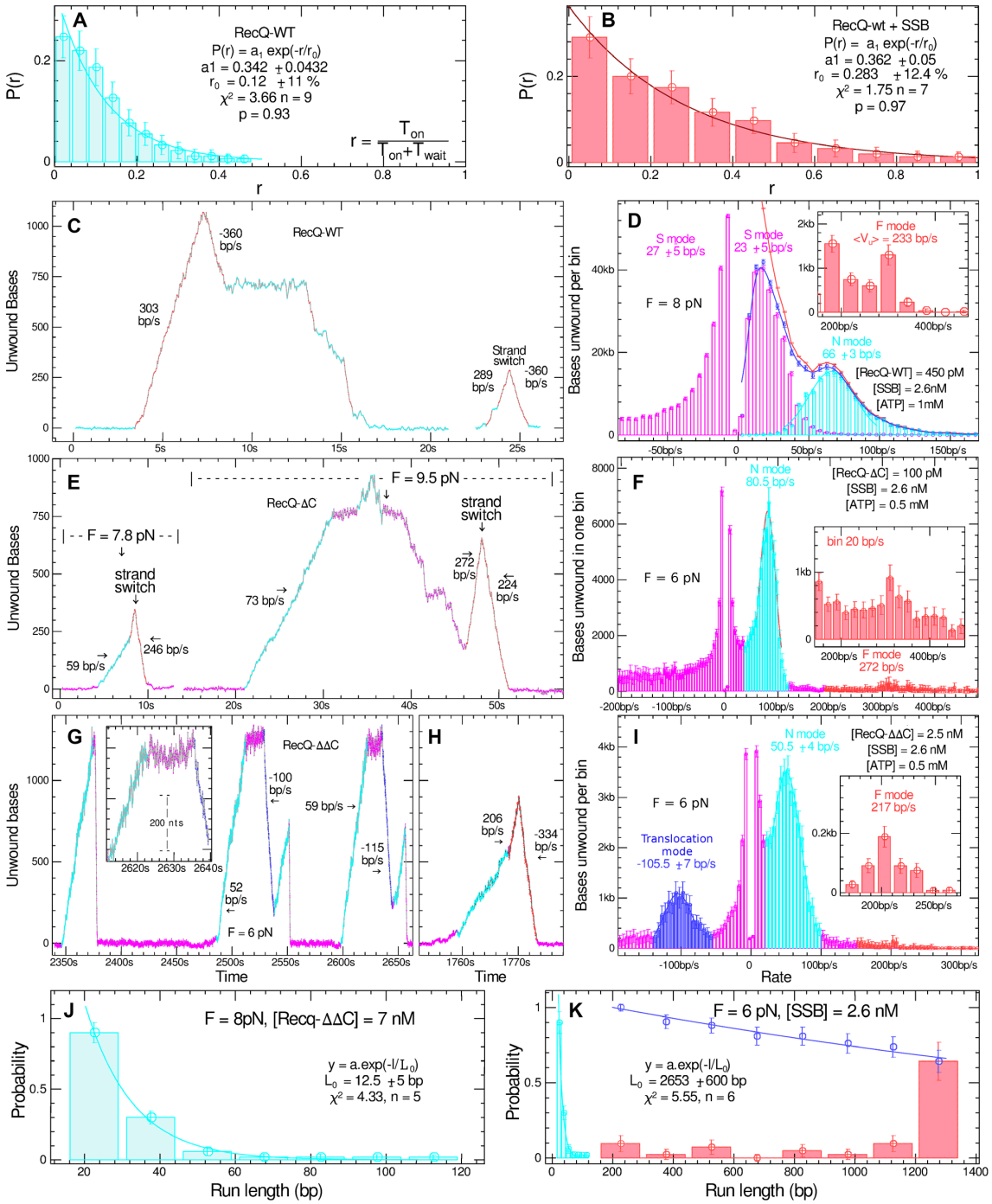

Figure 7. Interaction between SSB and RecQ. (**A** and **B**) SSB enhances the unwinding activity of RecQ-wt measured here by the ratio r of time duration during which the enzyme is active in a burst, T_{on}, to the total time separating the beginning of two consecutive bursts (T_{on} + T_{wait}), where T_{wait} is the waiting time separating bursts. The probability $P(r)$ of observing a ratio r is well fitted by an exponential function with a characteristic decay constant r_0, which increased from 0.12 ± 0.01 (A) to 0.283 ± 0.03 in presence of SSB (B). (**C**) Experimental unwinding traces of RecQ-wt in the presence of SSB ([RecQ-wt] = 450 pM, [ATP] = 0.5 mM). RecQ-wt displays enhanced rates (F mode) both during unwinding and translocation. (**D**) The histogram of RecQ-wt rate in presence of SSB, the diffusive mode is significantly reduced by a well-defined unwinding mode and a tail in the high rates corresponding to the fast mode of the helicase, which is better evidenced in the insert. (**E**) Experimental unwinding traces for RecQ-ΔC in the presence of SSB ([RecQ-ΔC] = 400 pM, [ATP] = 0.5 mM). RecQ-ΔC changes from N to F mode (with speed enhanced by a factor 4) both while unwinding or translocating. (**F**) The histogram for RecQ-ΔC, the fast mode is more pronounced and again leads to high rates, as shown in the insert. (**G**) Experimental unwinding trace for RecQ-ΔΔC in the presence of SSB ([RecQ-ΔΔC] = 2.5 nM, [ATP] = 0.5 mM). In these conditions, the enzyme fully unwinds the 1.2 kb hairpin. Notice that SSB increases the noise in the signal (see insert). (**H**) SSB also favors the fast mode of [RecQ-ΔΔC. (**I**) Histogram for RecQ-ΔΔC rate, where high rates are also seen (see insert) but in a relatively small number of events. In all cases, [SSB] = 2.6 nM. (**J** and **K**) Processivity histograms for RecQ-ΔΔC with the probability of events versus the unwound bases extend in the absence of SSB (J and blue histogram in K) and in the presence of SSB (K). The histograms are fitted to an exponential function $P(l) = \exp(-l/L_0)$ (with l the run length), which yields the processivity in the two cases, given by the parameter L_o in the figure.

rates: the previously observed S and N modes, and a new third mode that is about 4 times faster than the N mode (Figure 7D, Supplementary Table S3). The new fast (F) mode is observed in a small fraction of the unwinding events corresponding to 1.5% of all the bases unwound, meaning that over all the bases unwound by the helicase only 1.5% were unwound at a high rate (Insert of Figure 7D) and can be seen even at a low pulling force (∼3.5 pN). Careful inspection of the time-dependent DNA unwinding traces showed that the helicase can switch to the F mode during an unwinding event started in either the S or N mode (Figure 7C). When SSB is present, RecQ-wt in N mode also retains the ability to maintain the hairpin open by repetitive strand switches. If the unwinding is in the F mode, the enzyme is seen translocating on ssDNA after strand switching, maintaining the same rate. At [SSB] = 2.6 nM, the DNA is coated with SSB (66), therefore during reannealing RecQ translocates along ssDNA presumably by displacing SSB.

With RecQ-ΔC, SSB also enhances the helicase activity by 2-fold (Supplementary Table S3), and both the F and N modes are observed (Figure 7E-F), with the probability of the F mode being dependent on [SSB] (Supplementary Figure S13). In the F mode, strand switching is observed during unwinding, switching the enzyme to the translocation mode, a feature which is not observed in the N mode with RecQ-ΔC (Figure 7E).

Surprisingly, SSB strongly stimulates the unwinding activity of the RecQ-ΔΔC protein, with $K_A^{RecQ\text{-}\Delta\Delta C}/K_A^{RecQ\text{-}\Delta\Delta C+SSB} = 3$ (Figure 7G and Supplementary Table S3). Although RecQ-ΔΔC lacks the domain that contains an identified SSB binding site, in the presence of SSB, RecQ-ΔΔC switches from being an enzyme with very limited processivity to one that can unwind 1.2 kb (length of the DNA substrate) in a single run (Figure 7G). In these conditions, RecQ-ΔΔC also displays unwinding with a speed just slightly lower than the N mode of the RecQ-wt and also presents the F mode (Supplementary Table S3, and Figure 7H–I, insert). Moreover, RecQ-ΔΔC with SSB presents a strongly enhanced average processivity of 2.5 kb at 6 pN (Figure 7J–K). This unexpected result could point to a second catalytically relevant interaction between the helicase core domains of RecQ and SSB. The overall results support a model where the F kinetic mode, increased processivity, binding affinity, and strand switching are promoted by a complex RecQ/SSB association involving multiple interaction modes (see discussion below). SSB also leads to RecQ-ΔΔC translocating with a rate (105 ± 7 bp/s), two times faster than its unwinding rate, (Figure 7I). This difference is an indication of a passive mechanism of unwinding (44), suggesting that RecQ-ΔΔC is missing the structural element which makes RecQ-ΔC an active helicase.

To further test the molecular basis of SSB stimulation, a chimeric protein RecQ-Δ-SSB-C-ter fusion, in which RecQ-ΔC is fused to the flexible SSB-Ct, with 21 amino acid linker, was purified (Supplementary Figure S14). Interestingly, this fusion enzyme demonstrated a strongly enhanced overall unwinding activity, with $K_A^{RecQ\text{-}\Delta}/K_A^{RecQ\text{-}\Delta\text{-SSB-C-ter}} = 72$ (Supplementary Table S3), and an enhanced processivity compared to RecQ-ΔC (2.3 kb at $F = 6.3$ pN), but with nearly the same unwinding speed (Supplementary Figures S15 and S16). This is consistent with a multifaceted enhancement mechanism by SSB, in which the enhanced binding affinity and processivity come from the direct interaction of RecQ with the SSB-Ct, whereas the enhanced unwinding rate is the result of an interaction between the helicase core domains and a SSB domain different from the SSB-Ct. To gain better insight into the importance of SSB/RecQ interaction, SSB was replaced with T4 bacteriophage gp32 single-stranded binding protein, which binds ssDNA but lacks the SSB-Ct sequence, or a chimeric protein in which the *E. coli* SSB-Ct is fused onto gp32 (67) (Supplementary Figure S15). With 6 nM T4 gp32 (corresponding to its K_D), the unwinding activity of RecQ-ΔC is severely hindered, with $K_A^{RecQ(\Delta)}/K_A^{RecQ(\Delta)+gp32} = 0.14$ (Supplementary Table S3), which is likely due to gp32 competing with RecQ-ΔC for binding ssDNA. In contrast, with the gp32-SSB-Ct fusion protein RecQ-ΔΔC and RecQ-ΔC activity are nearly normal with $K_A^{RecQ\Delta}/K_A^{RecQ\Delta+gp32\text{-SSB-Ct}} = 0.55$ and $K_A^{RecQ\Delta\Delta}/K_A^{RecQ\Delta\Delta+gp32\text{-SSB-Ct}} = 0.5$ (Supplementary Table S3), but without inducing the F mode observed with full-length *E. coli* SSB. We have also investigated how RecQ opens a bubble in dsDNA linear molecule and unwinds it, obtaining similar results as in (68) (see Supplementary Figure S17).

DISCUSSION

The RecQ helicase architecture

RecQ proteins are defined by the presence of the helicase domain, the RecQ-C domain and, in most cases, the HRDC domain. Diverse functional roles in DNA processing have been proposed for each of these domains. We have used single-molecule studies to dissect the kinetics of DNA unwinding by the prototypical RecQ protein from *E. coli* and by variants that lack individual domains. Intuitively, one might assume that the RecQ helicase domain could function as a robust DNA unwinding construct in isolation. However, studies with two human RecQ proteins, RecQ1 and WRN (32,33,55) have indicated that the WH element from the RecQ-C domain is required for DNA unwinding. These studies have identified a dsDNA binding surface that is conserved in the WH domains of RecQ1 and WRN along with a β-hairpin 'pin' element that is critical for unwinding DNA. Surprisingly, mutational studies of the analogous β-hairpin in *E. coli* RecQ pointed to a far less prominent role for the pin in the bacterial enzyme, which leaves the role of the WH domain open (69). Consistent with a more peripheral role for the WH domain in *E. coli* RecQ, our study demonstrates that RecQ-ΔΔC, which lacks the WH and HRDC domains, presents helicase activity. However, we have also found that RecQ-ΔΔC has very limited unwinding activity in isolation due to its very weak ssDNA binding affinity and processivity. In contrast, adding the WH domain to the RecQ-ΔΔC protein (in the RecQ-ΔC enzyme) transforms the inefficient helicase domain into a very robust enzyme. An interesting feature shown in Figure 7I is that RecQ-ΔΔC with SSB displays a clear translocation rate of 105 bp/s, which is two times faster than its unwinding rate of 50 bp/s. This is a typical indication of a passive helicase (44). We interpret this result as the fact that deleting the WH domain switches the helicase from active to passive.

ssDNA and dsDNA binding sites play a crucial role in helicase activity

Many non-hexameric helicases are thought to function via inchworm-like mechanisms with (minimally) two DNA-binding sites within the helicase domain being used to translocate processively along a single strand of the duplex. The RecQ-ΔC protein possesses at least three DNA binding sites: ssDNA binding sites within each of the two lobes of the helicase domain and a dsDNA binding site in the WH domain (24). The DNA-bound structure RecQ-ΔC domain has shown that ssDNA passes between the two RecA domains, which constitute the motor unit, whereas the WH domain binds dsDNA (27). Support for this overall arrangement has also been provided by DNA-bound structures of eukaryotic RecQ proteins or domains (28–32,55,56). This domain arrangement for RecQ could help to explain the persistent strand-switching activity observed in our DNA hairpin unwinding assay with RecQ-wt and RecQ-ΔC. After the helicase has passed the apex of a DNA hairpin, ssDNA binding by the helicase domain (and possibly the WH domain) allows the protein to stay associated with the unwound DNA as it becomes a ssDNA translocase. While the enzyme continues tracking along the displaced strand, at the same time, the hairpin refolds behind the enzyme. The hairpin reformation in the wake of the enzyme induces the switching between ssDNA translocation and unwinding enzyme activities. This switching could be generated by the tension of hairpin reformation 'pulling' ssDNA out of the helicase domain cleft or due to RecQ binding to the elongating dsDNA.

Processivity of RecQ helicase increases with the force.

We find that RecQ-ΔC processivity increases exponentially with the applied force (Figure 3E). Interestingly, a recent theoretical study (70) predicted this behavior. The reason is that the helicase binding affinity for ssDNA is decreased by the pressure of the DNA fork. Applying a force and pulling apart the two DNA strands reduces the fork pressure and thus restores stable binding and improves the processivity. Our result thus provides the first validation of this theoretical work.

The role of the HRDC domain

When the HRDC domain is included with the helicase and RecQ-C domains (full-length protein), two specific features are observed. First, the RecQ-wt enzyme displays a persistent random walk unwinding mode (S mode) in addition to the continuous unwinding mode (N mode), and second, it provides loading capacity for three-way junction DNA, allowing unwinding without pre-existing ssDNA.

Recent bulk assays have shown that the presence of the HRDC domain inhibits both the ATPase rate and the translocation (or unwinding) rate of the RecQ-wt motor, without changing the tight coupling of 1 nt (or bp) per ATP hydrolyzed (39). However, those ensemble assays only reported averaged rates and could not detect the intrinsic RecQ dynamic heterogeneity that leads to the bimodal activity measured in this work. Harami *et al.* (39) propose that the HRDC mediates coordination of the RecA helicase domains, leading to the inhibition of the RecQ ATPase activity. This study used single molecule approaches to show that the HRDC domain produces a complex unwinding behavior when RecQ-wt unzips a hairpin in an unpeeling geometry. Furthermore, using a point mutant of the HRDC domain they showed that the complex behavior corresponding to our S-mode is abolished. This observation points towards an interaction of the HRDC domain with ssDNA. Our results support this scenario, but with additional information: the ability to switch between two modes probably relates to the binding of ssDNA with the HRDC domain leading to two different interaction modes. This could manifest in two ways: (i) upon binding, the HRDC domain transiently interacts with the motor core domains, suppressing ATPase activity and leading to slower translocation and unwinding (S mode) and (ii) on detaching from ssDNA, HRDC transiently decouples from the motor core domain, restoring the fastest ATPase activity and the normal unwinding and translocation rates (N mode) as observed in the absence of the HRDC domain (RecQ-ΔC). Recent single molecule studies on the Rep helicase (71) demonstrate how the helicase unwinding rate and processivity can be controlled by the conformation of a particular domain leading to different helicase modes, similar to that observed for RecQ-wt. The switching between different conformations may be a general mechanism for regulating the different activities of helicases. The RecQ three-way junction activity is consistent with the proposed role for the HRDC domain from the BLM RecQ helicase (28,65). Additional possible roles for the HRDC domain also exist. The HRDC domain could couple RecQ to other enzymes in a manner that modulates RecQ DNA unwinding activity. In the absence of a partner, this domain may adopt different configurations (with different orientation with respect the motor core domains) associated with the two unwinding regimes that we observe (S and N). The switch from the S persistent random walk mode to the N processive unwinding mode might also be induced by a change in the RecQ oligomeric state involving the HRDC domain. Precedent for alternative conformations of a helicase having different levels of helicase activity has recently been established for the UvrD DNA helicase (72). However, it is difficult to characterize the oligomeric state of RecQ in our single molecule experiments. Recent work of Rad *et al.* (68) has shown that working at RecQ concentrations ranging from 18 to 150 nM leads to the occurrence of a dimer or a higher oligomer that unwinds dsDNA at weak force. In our experiments, with 2–3 orders of magnitude lower RecQ concentration ranges, RecQ may be operating as a monomer. We observe a relatively well-defined rate in our helicase assay in the normal mode that corresponds to the asymptotic rate found in (64) at high RecQ concentrations (>80 nM). Future experiments combining fluorescence and single molecule manipulation with fluorescently labeled enzymes might allow following the RecQ unwinding activity, while simultaneously measuring the oligomerization state, or associated conformational changes, gaining insight into the nature of its bimodal behavior.

ssDNA translocation: S diffusive mode

Previous bulk studies have examined RecQ unwinding and ssDNA translocation but assumed that RecQ moves at a uniform rate (33,34,69). Our experimental system has revealed a complicated and non-uniform rate of DNA unwinding that challenges this assumption for RecQ-wt, which is also seen in (8). The bimodal nature of RecQ unwinding activity could help to explain the differences observed in previously published studies (33,34,69). Recent studies on RecQ helicases have also reported the presence of different modes for ssDNA translocation, including diffusive mode and a unidirectional mode (57). However, in contrast to our studies, the diffusion mode was only observed on ssDNA translocation activity, but not with DNA unwinding activity. The rich dynamics observed in the RecQ unwinding and translocation activity might account for the functional diversity present in this family of helicases.

The role of the interaction between RecQ and SSB

Many RecQ proteins work in complexes that include SSBs, topoisomerases, and other proteins. Previous NMR and bulk biochemical assays have shown that the *E. coli* RecQ WH domain interacts with the SSB-Ct tail and that this interaction stimulates RecQ DNA unwinding (21,22,34). In agreement with the recent single molecule approach (36), we confirmed that *E. coli* RecQ helicase activity is significantly altered by the presence of SSB and revealed a previously unknown complexity in this interaction. In one form, SSB-Ct enhances the overall activity of RecQ by increasing binding affinity and enzyme processivity. In a second form, SSB strongly enhances the RecQ enzymatic rate as would be predicted for allosteric activation induced by SSB binding. Consistent with the previous bulk studies (21), the introduction of a single mutation within the SSB-Ct abolishes the enhancement in RecQ unwinding activity. Moreover, adding the C-terminal eight residues from SSB to the gp32 protein (gp32-SSB-Ct fusion) stimulates RecQ activity. SSB and/or gp32-SSB-Ct fusion protein activity enhancement is observed with all three RecQ variants tested (RecQ-wt, RecQ-ΔC and RecQ-ΔΔC). The observed stimulation of helicase activity by SSB implies that the interaction producing this effect cannot rely solely within the WH domain since this domain is absent in RecQ-ΔΔC. The SSB effects observed with RecQ-wt, RecQ-ΔC and RecQ-ΔΔC are comparable (Supplementary Table S3). With the three enzymes, SSB enhancement is robust; it is more moderate with gp32-SSB-Ct fusion protein and disappears when the SSB-Ct sequence is altered. In the latter conditions (SSB-Ct variants), we observe an inhibition of the helicase activity, which could reflect a competition for binding ssDNA. SSB thus has two effects: first, it competes with the helicase for loading onto ssDNA, and second, it enhances the overall unwinding activity through improvements in binding affinity, unwinding rates and processivity. Previous biochemical assays have identified a binding site for SSB in the RecQ WH domain. Our findings with RecQ-ΔΔC support a model in which a second SSB binding site, which has not been identified, is present outside of the WH domain.

A second SSB-dependent effect concerns the helicase fast rate events, which are observed with RecQ-wt, RecQ-ΔC and RecQ-ΔΔC together with SSB-wt. The absence of F unwinding mode with SSB-ΔC1 or SSB-113 implies again that they rely on the SSB-Ct. But the SSB-Ct alone is apparently not sufficient to induce the F mode. Indeed, with the fusion protein that links RecQ-ΔC to the SSB-Ct, an enhancement of unwinding activity is observed but without the fast speed regime. The same observation holds for gp32-SSB-Ct fusion. We suspect that the F mode is triggered by interactions between the helicase domains of RecQ and SSB. In the recent work of Mills *et al.* (36), this fast mode was not reported, probably because fast rate events are very rare. The overall results support a model with at least two different binding modes between RecQ and SSB: (i) the previously described interaction between the WH domain and SSB-Ct, (ii) a second interaction between the helicase domain or the Zn^{2+}-binding domain and SSB, which is not restricted to the SSB-Ct and extends to other SSB domains.

How does SSB enhance RecQ activity? A partial answer has been given recently (36) where RecQ was shown to displace SSB bound to ssDNA. A simple model for activation can be formulated where SSB can act as a helicase loader since it binds ssDNA and provides a specific interaction region for RecQ that could help load the helicase. Since SSB has a strong affinity for ssDNA, some interesting questions arise: what occurs after the helicase has been loaded by SSB? Does the interaction between the two proteins remain as they travel together on ssDNA or does SSB stay at its original position while RecQ extrudes an ssDNA loop between the two proteins? Or does SSB dissociate as soon as the helicase starts unwinding the DNA? Although we cannot fully answer these questions, we can evaluate their consequences in our single molecule assay and give some insights on the mechanism.

A helicase loader activity for SSB would be predicted to increase the DNA unwinding functions of RecQ as we have seen. However, altering the helicase rates and processivity is more subtle. A possible mechanism is that the F mode and increased processivity are associated with a change in the conformation of the helicase domain. A related protein interaction-dependent enhancement mechanism exists for Upf1 helicase (73). By analogy with this mechanism, interaction with SSB could stabilize a conformation of RecQ that can unwind several hundred base pairs rapidly or that confers larger processivity. As SSB is initially bound on the ssDNA template, it is possible that a ssDNA loop could be extruded between RecQ and SSB. With the hairpin substrate under tension in this assay, extruding an ssDNA loop sequesters a portion of the template transiently until the enzyme dissociates, releasing the loop abruptly. We have observed a similar mechanism between the T4 replicative helicase and primase (45). No such evidence was observed with RecQ however. This would favor a second scenario in which RecQ and SSB travel together along ssDNA, which could drive the F mode and increase the processivity, as soon as RecQ starts unwinding.

SUPPLEMENTARY DATA

Supplementary Data are available at NAR Online.

ACKNOWLEDGEMENTS

This work has originated in collaboration with X.G. Xi. We wish to acknowledge stimulating discussions with Michelle Spiering and J.F. Allemand and their help with hairpins and ds-DNA constructs. Discussions with H. Le Hir, F. Fiorini, J. Ouellet, D. Bensimon, K. Neuman and R. Seidel are gratefully acknowledged. We also acknowledge the mechanical support to the experiment from C. Goncalves and J. Quintas.

Author Contributions: D.B., M.M. and V.C. did the single-molecule experiments and data analysis. K.A.M., W.Z. and B.D. prepared the RecQ enzymes. M.M.S. and D.B. prepared the DNA substrates. D.B., M.M., J.L.K., K.A.M., B.D. and V.C. wrote the paper.

FUNDING

European Research Council [MAGREPS 267 862 to V.C.]; Juan de la Cierva Program MICINN-JDC (to M.M); Science and Engineering Research Board grant [EMR/2016/003910 to D.B.]. The open access publication charge for this paper has been waived by Oxford University Press - *NAR* Editorial Board members are entitled to one free paper per year in recognition of their work on behalf of the journal.

Conflict of interest statement. V.C. is co-founder of PicoTwist.

REFERENCES

1. Umezu,K., Nakayama,K. and Nakayama,H. (1990) Escherichia coli RecQ protein is a DNA helicase. *Proc. Natl. Acad. Sci. U.S.A.*, **87**, 5363–5367.
2. Bennett,R.J. and Keck,J.L. (2004) Structure and function of RecQ DNA helicases. *Crit. Rev. Biochem. Mol.*, **39**, 79–97.
3. Khakhar,R. (2003) RecQ helicases: multiple roles in genome maintenance. *Trends Cell Biol.*, **13**, 493–501.
4. Handa,N., Morimatsu,K., Lovett,S.T. and Kowalczykowski,S.C. (2009) Reconstitution of initial steps of ds-DNA break repair by the RecF pathway of *E. coli*. *Genes Dev.*, **23**, 1234–1245.
5. Nakayama,H., Nakayama,K., Nakayama,R., Irino,N., Nakayama,Y. and Hanawalt,P.C. (1984) Isolation and genetic characterization of a thymineless death-resistant mutant of Escherichia coli " K12: Identification of a new mutation (recQ1) that blocks the RecF recombination pathway. *Mol. Gen. Genet.*, **195**, 474–480.
6. Courcelle,J. and Hanawalt,P.C. (1999) RecQ and RecJ process blocked replication forks prior to the resumption of replication in UV-irradiated Escherichia coli. *Mol. Gen. Genet.*, **262**, 543–551.
7. Hanada,K., Ukita,T., Kohno,Y., Saito,K., Kato,J. and Ikeda,H. (1997) RecQ DNA helicase is a suppressor of illegitimate recombination in Escherichia coli. *Proc. Natl. Acad. Sci. U.S.A.*, **94**, 3860–3865.
8. Harami,G.M., Seol,Y., In,J., Ferencziová,V., Martina,M., Gyimesi,M., Sarlós,K., Kovács,Z.J., Nagy,N.T., Sun,Y. *et al.* (2017) Shuttling along DNA and directed processing of D-loops by RecQ helicase support quality control of homologous recombination. *Proc. Natl. Acad. Sci. U.S.A.*, **114**, E466–E467.
9. Mohaghegh,P., Karow,J.K., Brosh,R.M. Jr, Bohr,V.A. and Hickson,I.D. (2001) The Bloom's and Werner's syndrome proteins are DNA structure-specific helicases. *Nucleic Acids Res.*, **29**, 2843–2849.
10. Hishida,T., Han,Y.W., Shibata,T., Kubota,Y., Ishino,Y., Iwasaki,H. and Shinagawa,H. (2004) Role of the Escherichia coli RecQ DNA helicase in SOS signaling and genome stabilization at stalled replication forks. *Genes Dev.*, **18**, 1886–1897.
11. Bachrati,C.Z. and Hickson,I.D. (2008) RecQ helicases: guardian angels of the DNA replication fork. *Chromosoma*, **117**, 219–233.
12. Karow,J.K., Wu,L. and Hickson,I.D. (2000) RecQ family helicases: roles in cancer and aging. *Curr. Opin. Genet. Dev.*, **10**, 32–38.
13. Harmon,F.G. and Kowalczykowski,S.C. (1998) RecQ helicase, in concert with RecA and SSB proteins, initiates and disrupts DNA recombination. *Genes Dev.*, **12**, 1134–1144.
14. Harmon,F.G., DiGate,R.J. and Kowalczykowski,S.C. (1999) RecQ helicase and topoisomerase III comprise a novel DNA strand passage function: a conserved mechanism for control of DNA recombination. *Mol. Cell*, **3**, 611–620.
15. Harmon,F.G., Brockman,J.P. and Kowalczykowski,S.C. (2003) RecQ helicase stimulates both DNA catenation and changes in DNA topology by topoisomerase III. *J. Biol. Chem.*, **278**, 42668–42678.
16. Suski,C. and Marians,K.J. (2008) Resolution of converging replication forks by RecQ and topoisomerase III. *Mol. Cell*, **30**, 779–789.
17. Brosh,R.M., Li,J.L., Kenny,M.K., Karow,J.K., Cooper,M.P., Kureekattil,R.P., Hickson,I.D. and Bohr,V.A. (2000) Replication protein A physically interacts with the Bloom's syndrome protein and stimulates its helicase activity. *J. Biol. Chem.*, **275**, 23500–23508.
18. MachweLozada,A.E., Wold,M.S., Li,G.M. and Orren,D.K. (2010) Molecular cooperation between the werner syndrome protein and replication protein a in relation to replication fork blockage. *J. Biol. Chem.*, **286**, 3497–3508.
19. Cejka,P., Cannavo,E., Polaczek,P., Masuda-sasa,T., Pokharel,S., Campbell,J.L. and Kowalczykowski,S.C. (2010) DNA end resection by Dna2-Sgs1-RPA and its stimulation by Top3-Rmi1 and Mre11-Rad50-Xrs2. *Nature*, **467**, 112–116.
20. Gangloff,S., Mcdonald,J.P., Bendixen,C., Arthur,L. and Rothstein,R. (1994) The yeast type I topoisomerase Top3 interacts with Sgsl, a DNA helicase Homolog: a potential eukaryotic reverse gyrase. *Microbiology*, **14**, 8391–8398.
21. Shereda,R.D., Bernstein,D.A. and Keck,J.L. (2007) A central role for SSB in *escherichiacoli* RecQ DNA helicase function. *J. Biol. Chem.*, **282**, 19247–1958.
22. Shereda,R.D., Reiter,N.J., Butcher,S.E. and Keck,J.L. (2009) Identification of the SSB binding site on *E. coli* RecQ reveals a conserved surface for binding SSB's C terminus. *J. Mol. Biol.*, **386**, 612–625.
23. Cobb,J.A., Bjergbaek,L., Shimada,K., Frei,C. and Gasser,S.M. (2003), DNA polymerase stabilization at stalled replication forks requires Mec1 and the RecQ helicase Sgs1. *EMBO J.*, **22**, 4325–4336.
24. Bernstein,D.A. and Keck,J.L. (2003) Domain mapping of Escherichia coli RecQ defines the roles of conserved N- and C-terminal regions in the RecQ family. *Nucleic Acids Res.*, **31**, 2778–2785.
25. Bernstein,D.A., Zittel,M.C. and Keck,J.L. (2003) High-resolution structure of the *E.coli* RecQ helicase catalytic core. *EMBO J.*, **22**, 4910–4921.
26. Bernstein,D.A. and Keck,J.L. (2005) Conferring substrate specificity to DNA helicases: role of the RecQ HRDC domain. *Structure*, **13**:1173–1182.
27. Manthei,K.A., Hill,M.C., Burke,J.E., Butcher,S.E. and Keck,J.L. (2015) Structural mechanisms of DNA bnding and unwinding in bacterial RecQ helicases. *Proc. Natl. Acad. Sci. U.S.A.*, **114**, 4292–4297.
28. Swan,M.K., Legris,V., Tanner,A., Reaper,P.M., Vial,S., Bordas,R., Pollard,J.R., Charlton,P.A., Golec,J.M. and Bertrand,J.A. (2014) Structure of human Bloom's syndrome helicase in complex with ADP and duplex DNA. *Acta Crystallogr. D Biol. Crystallogr.*, **70**, 1465–1475.
29. Pike,A.C., Gomathinayagam,S., Swuec,P., Berti,M., Zhang,Y., Schnecke,C., Marino,F., von Delft,F., Renault,L., Costa,A. *et al.* (2015) Human RECQ1 helicase-driven DNA unwinding, annealing, and branch migration: insights from DNA complex structures. *Proc. Natl. Acad. Sci. U.S.A.*, **112**, 4286–4291.
30. Newman,J.A., Savitsky,P., Allerston,C.K., Bizard,A.H., Özer,Ö., Sarlós,K., Liu,Y., Pardon,E., Steyaert,J., Hickson,I.D. *et al.* (2015) Crystal structure of the Bloom's syndrome helicase indicates a role for the HRDC domain in conformational changes. *Nucleic Acids Res.*, **43**, 5221–5235.
31. Gyimesi,M., Harami,G.M., Sarlós,K., Hazai,E., Bikádi,Z. and Kovács,M. (2012) Complex activities of the human Bloom's syndrome helicase are encoded in a core region comprising the RecA and Zn-binding domains. *Nucleic Acids Res.*, **40**, 3952–3963.
32. Pike,A.C.W., Shrestha,B., Popuri,V., Burgess-Browna,N., Muzzolini,L., Costantini,S., Vindigni,A. and Gileadi,O. (2008)

Structure of the human RECQ1 helicase reveals a putative strand-separation pin. *Proc. Natl. Acad. Sci. U.S.A.*, **106**, 1039–1044.
33. Lucic,B., Zhang,Y., King,O., Mendoza-Maldonado,R., Berti,M., Niesen,F.H., Burgess-Brown,N.A., Pike,A.C.W., Cooper,C.D.O., Gileadi,O. *et al.* (2011) A prominent β-hairpin structure in the winged-helix domain of RECQ1 is required for DNA unwinding and oligomer formation. *Nucleic Acids Res.*, **39**, 1703–1717.
34. Killoran,M.P. and Keck,J.L. (2006) Sit down, relax and unwind: structural insights into RecQ helicase mechanisms. *Nucleic Acids Res.*, **34**, 4098–4105.
35. Shereda,R.D., Kozlov,A.G., Lohman,T.M., Cox,M.M. and Keck,J.L. (2008) SSB as an Organizer/Mobilizer of genome maintenance complexes. *Crit. Rev. Biochem. Mol. Biol.*, **43**, 289–318.
36. Mills,M., Harami,G.M., Seol,Y., Gyimesi,M., Martina,M., Kovács,Z.J., Kovács,M. and Neuman,K.C. (2017) RecQ helicase triggers a binding mode change in the SSB-DNA complex to efficiently initiate DNA unwinding. *Nucleic Acids Res.*, **45**, 11878–11890.
37. Rad,B. and Kowalczykowski,S.C. (2012) Efficient coupling of ATP hydrolysis to translocation by RecQ helicase. *Proc. Natl. Acad. Sci. U.S.A.*, **109**, 1443–1448.
38. Sarlós,K., Gyimesi,M. and Kovács,M. (2012) RecQ helicase translocates along single-stranded DNA with a moderate processivity and tight mechanochemical coupling. *Proc. Natl. Acad. Sci. U.S.A.*, **109**, 9804–9809.
39. Harami,G.M., Nagy,N.T., Martina,M., Neuman,K.C. and Kovács,M. (2015) The HRDC domain of *E. coli* RecQ helicase controls single stranded DNA translocation and double-stranded DNA unwinding rates without affecting mechanoenzymatic coupling. *Sci. Rep.*, **5**, 11091.
40. Greenleaf,W.J., Woodside,M.T. and Block,S.M. (2007) High resolution, single-molecule measurements of biomolecular motion. *Annu. Rev. Biophys. Biomol. Struct.*, **36**, 171–190.
41. Tanner,N.A. and Van Oijen,A.M. (2010) Visualizing DNA replication at the single-molecule level. *Meth. Enzymol.*, **475**, 259–277.
42. Dessinges,M.N., Lionnet,T., Xi,X.G., Bensimon,D. and Croquette,V. (2004) Single-molecule assay reveals strand switching and enhanced processivity of UvrD. *Proc. Natl. Acad. Sci. U.S.A.*, **101**, 6439–6444.
43. Lionnet,T., Spiering,M.M., Benkovic,S.J., Bensimon,D. and Croquette,V. (2007) Real-time observation of bacteriophage T4 gp41 helicase reveals an unwinding mechanism. *Proc. Natl. Acad. Sci. USA*, **104**, 19790–19795.
44. Manosas,M., Xi,X.G., Bensimon,D. and Croquette,V. (2010) Active and passive mechanisms of helicases. *Nucleic Acids Res.*, **38**, 5518–5126.
45. Manosas,M., Spiering,M.M., Zhuang,Z., Benkovic,S.J. and Croquette,V. (2009) Coupling DNA unwinding activity with primer synthesis in the bacteriophage T4 primosome. *Nat. Chem. Biol.*, **5**, 904–912.
46. Manosas,M., Perumal,S.K., Croquette,V. and Benkovic,S.J. (2012) Direct observation of stalled fork restart via fork regression in the T4 replication system. *Science*, **338** , 1217–1220.
47. Gosse,C. and Croquette,V. (2002) Magnetic tweezers: micromanipulation and force measurement at the molecular level. *Biophysical J.*, **82**, 3314–3329.
48. Kocsis,Z.S., Sarlós,K., Harami,G.M., Martina,M. and Kovacs,M. (2014) A Nucleotide-dependent and HRDC Domain-dependent structural transition in DNA-bound RecQ helicase. *JBC*, **289**, 5938.
49. George,N.P., Ngo,K.V., Chitteni-Pattu,S., Norais,C.A., Battista,J.R., Cox,M.M. and Keck,J.L. (2012) Structure and cellular dynamics of Deinococcus radiodurans Single-stranded DNA (ssDNA)-binding protein (SSB)-DNA complexes. *J. Biol. Chem.*, **287**, 22123–22132
50. Strick,T.R., Allemand,J.-F., Bensimon,D., Bensimon,A. and Croquette,V. (1991) The elasticity of a single supercoiled DNA molecule. *Science*, **271**, 1835–1837.
51. Chung,S.H. and Kennedy,R.A. (1991) Forward and backward non-linear filtering technique for extracting small biological signals from noise. *J. Neurosci. Methods*, **40**, 71–86.
52. Harmon,F.G. and Kowalczykowski,S.C. (2001) Biochemical characterization of the DNA helicase activity of the escherichia coli RecQ helicase. *J. Biol. Chem.*, **276**, 232–243.
53. Zhang,X.-D., Dou,S.-X., Xie,P., Hu,J.-S., Wang,P.-Y. and Xi,X.G. (2006) Escherichia coli recq is a rapid, efficient, and monomeric helicase. *J. Biol. Chem.*, **281**, 12655–12663.
54. Huber,M.D., Duquette,M.L., Shiels,J.C. and Maizels,N. (2006) A conserved G4 DNA binding domain in RecQ family helicases. *J. Mol. Biol.*, **358**, 1071–1080.
55. Kitano,K., Kim,S.Y. and Hakoshima,T. (2010) Structural basis for DNA strand separation by the unconventional winged-helix domain of RecQ helicase WRN. *Structure*, **18**, 177–187.
56. Yodh,J.G., Stevens,B.C., Kanagaraj,R., Janscak,P. and Ha,T. (2009) BLM helicase measures DNA unwound before switching strands and hRPA promotes unwinding reinitiation. *EMBO J.*, **28**, 405–416.
57. Klaue,D., Kobbe,D., Kemmerich,F., Kozikowska,A., Puchta,H. and Seidel,R. (2013) Fork sensing and strand switching control antagonistic activities of RecQ helicases. *Nat. Commun.*, **4**, 2024.
58. Fiorini,F., Bagchi,D., Le Hir,H. and Croquette,V. (2015) Human Upf1 is a highly processive RNA helicase and translocase with RNP remodelling activities. *Nat. Commun.*, **6**, 7581
59. Wang,S., Qin,W., Li,J.H., Lu,Y., Lu,K.Y., Nong,D.G., Dou,S.X., Xu,C.H., Xi,X.G. and Li,M. (2015) Unwinding forward and sliding back: an intermittent unwinding mode of the BLM helicase. *Nucleic Acids Res.*, **43**, 3736–3746.
60. Budhathoki,J.B., Stafford,E.J., Yodh,J.G. and Balci,H. (2015) ATP dependent G-quadruplex unfolding by Bloom helicase exhibits low processivity. *Nucleic Acids Res.*, **43**, 5961–5970.
61. Roy,R., Kozlov,A.G., Lohman,T.M and Ha,T. (2009) SSB protein diffusion on single-stranded DNA stimulates RecA filament formation. *Nature*, **461**, 1092–1097.
62. Ha,T., Kozlov,A.G. and Lohman,T.M. (2012) Single-molecule views of protein movement on single-stranded DNA. *Annu. Rev. Biophys.*, **41**, 295–319.
63. Senavirathne,G., Jaszczur,M., Auerbach,P.A., Upton,T.G., Chelico,L., Goodman,M.F. and Rueda,D. (2012) Single-stranded DNA scanning and deamination by APOBEC3G cytidine deaminase at single molecule resolution. *J. Biol. Chem.*, **287**, 15826–15835.
64. Lee,K.S., Balci,H., Jia,H., Lohman,T.M. and Ha,T. (2013) Direct imaging of single UvrD helicase dynamics on long single-stranded DNA. *Nat. Commun.*, **4**, 1878.
65. Wu,L., Chan,K.L., Ralf,C., Bernstein,D.A., Garcia,P.L., Bohr,V.A., Vindigni,A., Janscak,P., Keck,J.L. and Hickson,I.D. (2005) The HRDC domain of BLM is required for the dissolution of double Holliday junctions. *EMBO J.*, **24**, 2679–2687.
66. Hatch,K., Danilowicz,C., Coljee,V. and Prentiss,M. (2007) Direct measurements of the stabilization of single-stranded DNA under tension by single-stranded binding proteins. *Phys. Rev. E.*, **76**, 021916.
67. Lu,D., Myers,A.R., George,N.P. and Keck,J.L. (2011) Mechanism of exonuclease I stimulation by the single-stranded DNA-binding protein. *Nucleic Acids Res.*, **39**, 6536–6545.
68. Rad,B., Forgeta,A.L., Baskinb,R.J. and Kowalczykowski,S.C. (2015) Single-molecule visualization of RecQ helicase reveals DNA melting, nucleation, and assembly are required for processive DNA unwinding. *Proc. Natl. Acad. Sci. U.S.A.*, **112**, E6852–E6861.
69. Vindigni,A., Marino,F. and Gileadi,O. (2010) Probing the structural basis of RecQ helicase function. *Biophys. Chem.*, **149**, 67–77.
70. Pincus,D.L., Chakrabarti,S. and Thirumalai,D. (2015) Helicase processivity and not the unwinding velocity exhibits universal increase with force. *Biophys J*, **109**, 220–230.
71. Arslan,S., Khafizov,R., Thomas,C.D., Chemla,Y.R. and Ha,T. (2015) Engineering of a superhelicase through conformational control. *Science*, **348**, 344–347.
72. Comstock,M.J., Whitley,K.D., Jia,H., Sokoloski,J., Lohman,T.M., Ha,T. and Chemla,Y.R. (2015) Direct observation of structure-function relationship in a nucleic acid–processing enzyme. *Science*, **348**, 352–354.
73. Chamieh,H., Ballut,L., Bonneau,F. and Le Hir,H. (2008) NMD factors UPF2 and UPF3 bridge UPF1 to the exon junction complex and stimulate its RNA helicase activity. *Nat. Struct. Mol. Biol.*, **15**, 85–93.